

## Investigation of the Brazil Current front variability from altimeter data

Gustavo J. Goni

Atlantic Oceanographic and Meteorological Laboratory, U.S. Department of Commerce, National Oceanic and Atmospheric Administration, Miami, Florida

Ilana Wainer

Physical Oceanography Department, University of Sao Paulo, Sao Paulo, Brazil

**Abstract.** The southwestern Atlantic Ocean is characterized by the confluence of the Brazil and Malvinas Currents, which form very strong surface and subsurface fronts that can be detected from hydrographic and remote sensing observations. Three data sets, consisting of TOPEX/Poseidon-derived sea height anomalies, the climatologically derived depth of the 10°C isotherm, and reduced gravity, are used in conjunction with a two-layer dynamical ocean scheme to monitor the Brazil Current front and to investigate its variability during a 6 year period (1993–1998). Results reveal that the fronts exhibit motions that are larger zonally than meridionally, showing strong interannual variability with annual mean amplitudes that range from 1° to 6°. The annual and semiannual components account for more than 75% of the variability of the frontal oscillations. In the annual cycle the frontal motions appear to be related closely to fluctuations in the baroclinic transport of the Brazil Current and are only influenced by the Malvinas Current when the Brazil Current transport is very small.

### 1. Introduction

The upper ocean circulation in the southwestern Atlantic is dominated by the presence of the warm and salty southward flowing Brazil Current (BC) and the cold and relatively fresh northward flowing Malvinas Current (MC) (Figure 1). The BC, the western boundary current associated with the subtropical gyre in the South Atlantic, turns southeast at ~38°S [Olson *et al.*, 1988], sheds warm rings with length scales of 400–500 km [Roden, 1986], and meanders back toward the north. Three water masses are found in the upper thousand meters in this region [Maamaatuaiahutapu *et al.*, 1992]. The Thermocline Water, of subtropical origin and carried by the BC, is mostly confined to the continental break [Garfield, 1990]. This water is characterized by a strong and deep thermocline with marked spatial and temporal variability. The Subantarctic Surface Water, which is carried by the MC, meets the Thermocline Water in the upper 800 m, flows beneath the thermocline [Gordon, 1981], and forms the Antarctic Intermediate Water, 500–1000 m deep, which recirculates with the subtropical gyre [Maamaatuaiahutapu *et al.*, 1998]. The region of convergence of these two currents, called the confluence [Gordon and Greengrove, 1986], exhibits very complex frontal motions and patterns with the simultaneous presence of warm and cold eddies. However, these two currents do not always collide, as there is evidence that leakage of water of the MC mixes with water from the continental shelf and the Rio de La Plata discharge, flowing northward on the continental shelf break and east of the BC waters [Lentini *et al.*, 2001; Piola *et al.*, 2000; Sunye and Servain, 1998]. The strong surface thermal front in the confluence region is characterized by the contrasting prop-

erties of the Thermocline and Subantarctic Surface Water masses. In situ estimates indicate that this frontal region can have horizontal gradients of up to 1°C(250 m)<sup>-1</sup> [Garzoli and Garraffo, 1989]. Hydrographic measurements also reveal that these frontal regions are associated with strong subsurface horizontal thermal gradients, which, in turn, can be related to the depth of a given isotherm [Roden, 1986; Garzoli and Garraffo, 1989].

The spatial characteristics of the variability of this frontal region have been studied by investigating the location of the separation of the BC from the continental margin [Olson *et al.*, 1988] and the changes in the geometry of the front [Garzoli *et al.*, 1992]. The time variability of the BC front occurs over scales that range from a few days [Garzoli and Garraffo, 1989] to interannual. Legeckis and Gordon [1982] and Gordon [1989] showed from advanced very high resolution radiometer (AVHRR) imagery that the BC frontal oscillations have periods of ~2 months. Estimates of the motion of the BC front using a 1 year inverted echosounder data record also revealed the existence of oscillations with periods of 2 months, probably related to the north-south motions of the BC, and of 12 months associated with the penetration of the MC [Garzoli and Garraffo, 1989].

In general, the large-scale curl of the wind stress is the major forcing mechanism of the upper ocean. Wainer *et al.* [2000] used numerical modeling to show that the wind stress computed over a region in the South Atlantic is an important factor to consider in the investigation of the motion of the BC front. Moreover, the relative strength of the BC and MC transports has also been recognized to be of key importance in the confluence region as they are linked to the location and motion of the front [Agra and Nof, 1993; Lebedev and Nof, 1996]. The annual cycle of the BC frontal motion has been linked to variability in the strength of both the BC [Provost *et al.*, 1992],

Copyright 2001 by the American Geophysical Union.

Paper number 2000JC000396.  
0148-0227/01/2000JC000396\$09.00

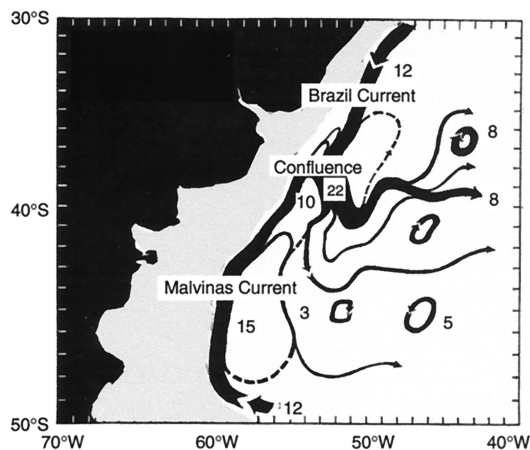


**Figure 1.** Schematic of the geostrophic time-averaged mass transport of the upper 1000 m in the western Argentine Basin based on the hydrographic data collected within the Confluence Project. The numbers indicate transports in sverdrups referenced to 1000 m depth [adapted from *Confluence Principal Investigators*, 1990].

which is forced by winds in the subtropics with a dominant annual period, and the MC, which has been suggested to be linked to the semiannual atmospheric forcing over the Southern Ocean [Large and van Loon, 1989; F. Vivier et al., Remote and local forcing in the Brazil-Malvinas region, submitted to *Journal of Physical Oceanography*, 2001, hereinafter referred to as Vivier et al., submitted manuscript, 2001]. Results from numerical modeling also confirm that the variability of the confluence is partly linked to transport changes of the MC and BC [Matano et al., 1993]. This last study concluded that (1) the BC intensified while the MC weakened during the austral summer, causing a southern displacement of the confluence, and (2) these conditions were reversed during the winter months when the confluence exhibited a shift to the north. These results also appear in the coupled general circulation model (GCM) simulation [Wainer et al., 2000] where the seasonal cycle in transport associated with both the BC and MC and the frontal meridional displacement are closely linked to the seasonal variations in the local wind stress curl. Numerical experiments using a simple hydrodynamic model reveal that the separation of the BC from the continental margin is highly dependent on the BC and MC transports [Matano, 1993]. However, results from a recent study combining TOPEX/Poseidon (T/P) and current meter observations reveal that the influence of the MC transport in the annual migration of the confluence may be marginal, although still of importance in the semiannual component [Vivier and Provost, 1999].

This work will also focus on the investigation of the local ocean forcing, namely, the variability of transport of the BC and MC, and on the motion of the BC front. Therefore the monitoring of these transports is key to this study. Maamaatuaiahutapu et al. [1998] present a partial list of transport estimates for these two currents computed using a wide variety of methods. The transports exhibit a large range of values, depending on the reference depth, location, and methodology used. Sustained observations suitable for investigating long-term variability in the dynamics of the confluence region are limited to remote sensing procedures. The lack of availability of continuous long-term hydrographic observations makes al-

timetry and AVHRR satellite-derived data very useful tools to investigate the time and space variability of the frontal dynamics. The longest available time series of volume transport of the MC and BC are derived from altimetry and current meter measurements. Long-term monitoring of these current transports shows that the MC exhibits values ranging from 12 to 47 Sv [Vivier and Provost, 1999] and that the BC exhibits values of up to 20 Sv [Goni et al., 1996]. The AVHRR-derived sea surface temperature daily images, which reflect the thermal conditions in a very thin layer of the upper ocean, have been used to identify strong temperature gradients associated with the surface front [Olson et al., 1988]. However, it has been observed that this thin layer sometimes exhibits only a weak relationship with the upper ocean dynamic conditions. On the other hand, sea height anomalies obtained from altimetry provide information about the dynamics in the upper hundred meters, which are in part related to mesoscale processes in the confluence region [Provost and Le Traon, 1993; Goni et al., 1996]. Therefore the BC frontal location can be investigated in terms of the position of the main thermocline, which is closely related to the upper ocean dynamics. The variability of the depth of two isotherms, 8° and 10°C, which are associated with the main thermocline, has been linked to the dynamic height anomaly referenced to 1500 m [Gordon, 1989; Garzoli and Garraffo, 1989]. The location at which these two isotherms are found at ~200 m depth has also been linked to the location of the surface and subsurface fronts [Garzoli and Garraffo, 1989].

Previous research has shown that altimeter-derived sea height anomaly data used in combination with climatological hydrographic data can be used to monitor the depth of isotherms that lie within the Thermocline Waters [Goni et al., 1996]. The objective of the present study is to use the methodology described by Goni et al. [1996] to monitor the variability of the BC front and to investigate the link between the BC and MC transports with the frontal variability. These objectives are accomplished by investigating four parameters: (1) the frontal time density, a measure of the probability of finding a front at a given location, (2) the latitude where the BC front separates from the continental margin, (3) the southernmost location of the fronts, and (4) the BC transport.

## 2. Data

### 2.1. Altimeter Data

The T/P-derived sea height anomaly,  $\eta'(x, y, t) = \eta(x, y, t) - \bar{\eta}(x, y)$ , is the deviation of the actual sea height  $\eta$  referred to the mean sea height  $\bar{\eta}$ , usually computed over a period of time of several years. The T/P altimeter measures the sea height anomaly along groundtracks, which are separated 3° zonally, approximately every 9.91 days. The data used in this study were processed with the standard altimetric corrections with the sea height anomaly values referenced to the 1993–1998 mean and interpolated into a 9 km alongtrack grid [Cheney et al., 1994]. The sea height anomaly during the study period ranges between -0.6 and 0.6 m and has a standard deviation of ~0.2 m. The space-time diagram along the ascending T/P groundtrack *a323* (Figure 2) reveals that most of the variability along this groundtrack (Plate 1a) is restricted to latitudes between 35° and 40°S, with a strong year to year difference as shown by the very low sea height anomaly values found during 1993 and very high values during 1998. The largest variability is found at 38°S (Plates 1a and 1b). The space-time diagram for the descending T/P groundtrack *d294*

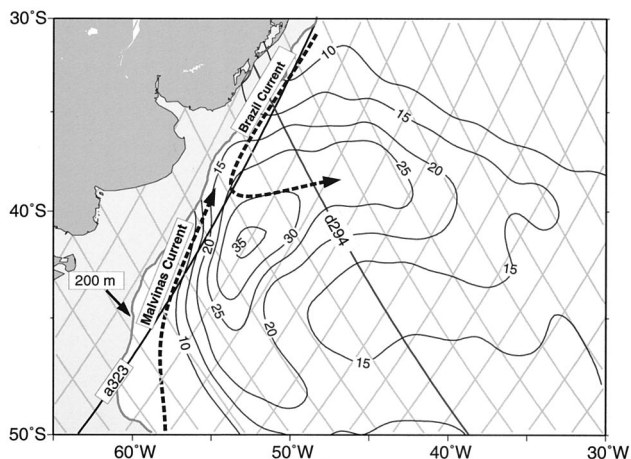


**Figure 2.** The rms of the sea height (contours). The altimeter groundtracks (thin shaded lines, except for  $d294$  and  $a323$ , which are shown in black) and the 200 m isobath are superimposed. The selected groundtrack  $d294$  (black line) is used to estimate the baroclinic transport of the BC, while  $a323$  is used to investigate the separation of the BC from the continental margin. The lightly shaded area shows the Argentinean continental shelf.

(Figure 2) shows that the maximum sea height rms value along this groundtrack is also found at 38°S (Plate 1d).

Geosat-derived sea height anomaly maps in the confluence area revealed that there is a spatial alternation of positive and negative sea height anomaly values that run in the same direction as the continental margin. This alternation of values has been reported to be caused by the semiannual component of the motion of the BC front and by Rossby waves, which can have sea height anomalies of up to 0.4 m [Provost and Le Traon, 1993]. The rms values of the sea height range from  $\sim 0.1$  to 0.35 m (Figure 2). The larger rms values are associated with the sea height variability in the Brazil-Malvinas Confluence region, mainly because of frontal movements and ring dynamics. The lower values, off the Argentinean continental margin, are associated with the less variable MC.

## 2.2. Climatological Data

Climatological temperature and salinity data in a  $1^\circ \times 1^\circ$  grid [Conkright *et al.*, 1998] are used to compute the mean upper layer thickness and the mean reduced gravity (Figure 3). The uncertainty of this climatological data is given by the standard deviation of the data used for these estimates [Levitus, 1982]. The upper layer thickness, as defined in this study, goes from the sea surface to the depth of the 10°C isotherm, which can be associated with the location of the main thermocline or boundary between the Thermocline and the Antarctic Intermediate Water. The mean reduced gravity  $g'$  is estimated using the mean upper and lower layer densities:

$$g'(x, y) = \varepsilon(x, y)g(y) = \frac{\rho_2(x, y) - \rho_1(x, y)}{\rho_2(x, y)} g(y), \quad (1)$$

where  $g$  is the acceleration of gravity and  $\rho_1$  and  $\rho_2$  are the mean densities of the upper and lower layers, respectively. The parameter  $\varepsilon$ , and hence  $g'$ , provides a measure of the vertical stratification in the region. The region between 40° and 50°W and 40° and 45°S, which is away from the region affected by the presence of warm rings (C. Lentini *et al.*, Warm ring dynamics

in the Brazil-Malvinas Confluence zone from TOPEX/Poseidon satellite altimeter data, submitted to *Journal of Marine Research*, 2001, hereinafter referred to as Lentini *et al.*, submitted manuscript, 2001), is characterized by the strongest contrast. This contrast becomes weaker close to the continental margin because of the influence of the rather vertically homogeneous MC [Maamaatuaiahutapu *et al.*, 1992].

## 3. Two-Layer Model

The merging of the subtropical waters of the BC with the subpolar waters of the MC results in a marked contrast in vertical stratification. As a first approximation, this vertical stratification of the ocean can be described using a two-layer reduced gravity ocean scheme [Goni *et al.*, 1996]. In a two-layer model the upper layer thickness  $h_1$  is

$$h_1(x, y, t) = \bar{h}_1(x, y) + h'_1(x, y, t) = \bar{h}_1(x, y) + \frac{1}{\varepsilon(x, y)} \times [\eta'(x, y, t) - B'(x, y)], \quad (2)$$

where  $\bar{h}_1$  is the mean upper layer thickness,  $h'_1$  is the deviation, or anomaly, of the upper layer thickness with respect to its mean value, and  $B'$  is the barotropic contribution to the sea height anomaly.  $|B'|$  in this region, where  $\bar{B}' = 0$ , has been shown to be much smaller than  $|\eta'|$  [Goni *et al.*, 1996] and will be disregarded in this study. The space-time diagram of upper layer thickness for the ascending T/P groundtrack  $a323$  obtained using (2) is shown in Plate 1c. This field exhibits large variability associated with frontal movements and the passage of warm and cold rings. The latitude of maximum rms value is also superimposed on Plate 1c.

The baroclinic transport between two locations,  $x_b$  and  $x_c$  centered at  $(x_a, y_a)$ , across an altimeter groundtrack  $S_{cl}$  can be found if the bottom layer is assumed to be at rest [Goni *et al.*, 1996]:

$$S_{cl}(x_a, y_a, t) = \frac{g'(x_a, y_a)}{2f(y_a)} \Delta h_1^2(x_a, y_a, t), \quad (3)$$

where  $\Delta h_1^2(t, x_a, y_a)$  is the difference of the square of the upper layer thicknesses between the two locations and  $f$  is the Coriolis parameter. Estimates of upper layer thickness and transports obtained using this methodology were validated using simultaneous Geosat and inverted echosounder data during 1986–1989 [Goni *et al.*, 1996]. These results showed that the upper layer thickness anomaly associated with the passage of warm rings and the BC had values that ranged from  $-300$  to 300 m, associated with baroclinic transport variations of up to 40 Sv.

## 4. Results

The variability of the confluence region is investigated as a function of the spatial and temporal variability of the location of the BC front, defined here as the location where the 10°C isotherm is 200 m deep [Garzoli and Bianchi, 1987]. The BC front, as defined in this study, has been associated with strong horizontal thermal gradients at the surface and at subsurface levels from hydrographic data [Roden, 1986]. Three different parameters obtained from the altimeter-derived upper layer thickness maps, which characterize the geometry of the BC front, are analyzed here: (1) the frontal time density, (2) the

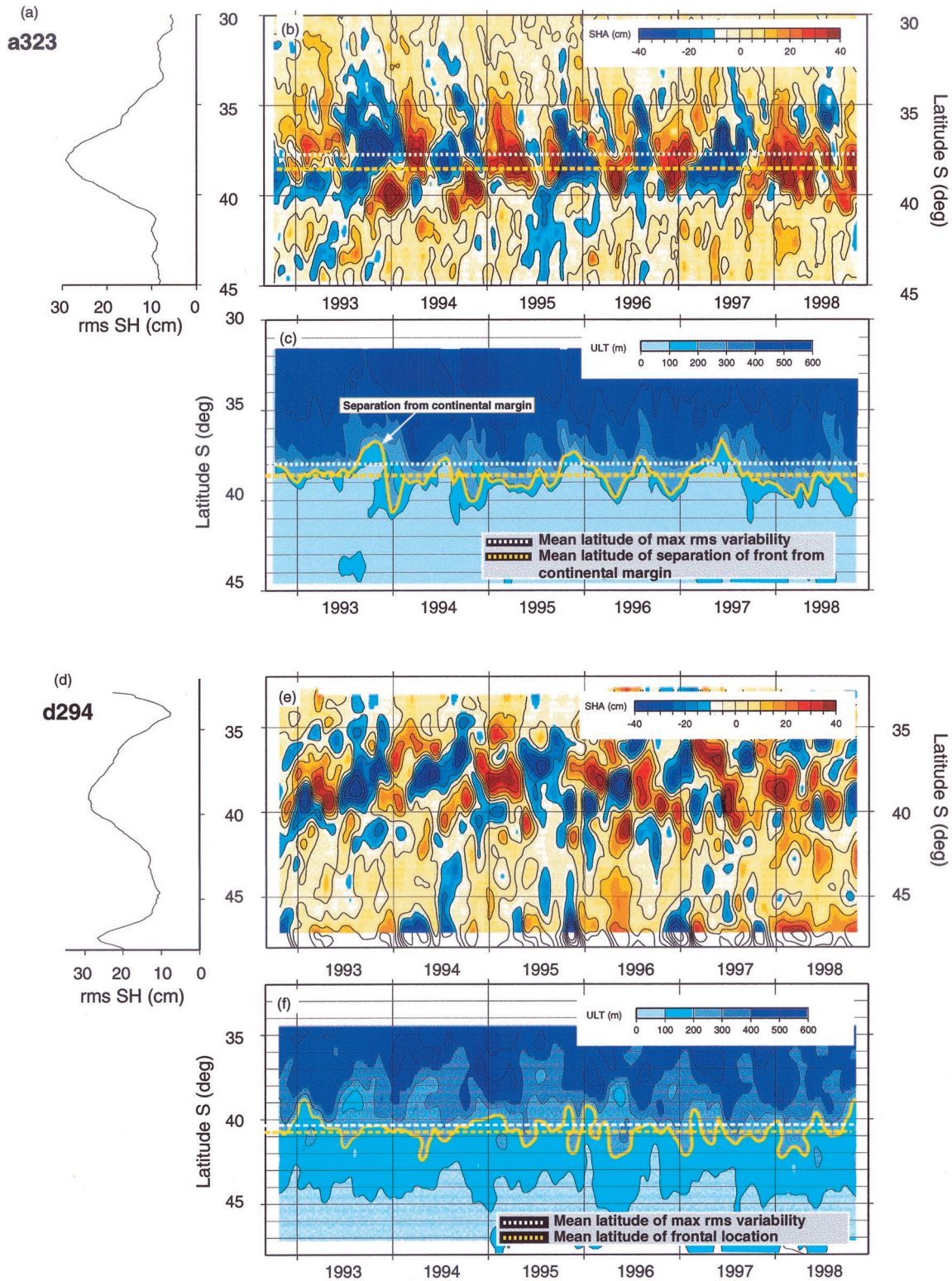


**Plate 1.** (a) The rms of the sea height along T/P ascending groundtrack *a323* (Figure 2). (b) Space-time diagram of the sea height anomaly along the same groundtrack. Contours are drawn every 0.1 m. Values range from  $-0.6$  to  $0.6$  m, with a standard deviation of  $\sim 0.1$  m. Most of the variability is between  $35^{\circ}$  and  $40^{\circ}$ S. The near-zero values (yellows) outside of this region correspond to regions of lesser variability. The annual cycle is partly shown by the alternation of the positive (reds) and negative (blues) sea height anomaly values. The dotted white line (Plates 1b and 1c) indicates the latitude of maximum rms value along the altimeter groundtrack, while the dotted yellow line shows the mean latitude of the front, which, along this groundtrack, is associated with the separation of the BC front from the continental shelf break. (c) Space-time diagram of the altimeter-derived upper layer thickness along the same groundtrack. The 200 m contour corresponding to the separation of the BC front from the continental margin is superimposed. (d), (e), and (f) Same as Plates 1a, 1b, and 1c except for T/P descending groundtrack *d294*. The yellow dotted line here shows the mean location of the BC front.

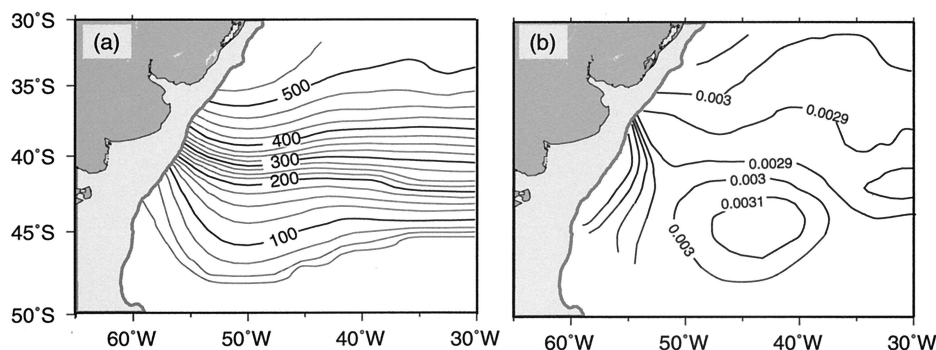


**Figure 3.** Climatologically derived (a) depth of the 10°C isotherm in meters and (b)  $\varepsilon$  (nondimensional), where  $\varepsilon = g'/g$ . The light shading corresponds to the continental shelf.

separation of the BC front from the continental margin, and (3) the southernmost location of the BC front.

The region of study is anisotropic [Provost and Le Traon, 1993], and meridional variations of velocity (and hence of sea height) are up to 3 times higher than zonal values. Therefore a Gaussian interpolator of radius  $1/6^\circ$  meridionally and  $1/4^\circ$  zonally is used to construct the sea height anomaly maps in a regular  $1/4^\circ$  grid. Maps of normalized errors, defined as the variance divided by the field variance, show larger values inside the diamond region between altimeter groundtracks [Goni *et al.*, 1996]. The sea height anomaly, mean upper layer thickness, and reduced gravity fields are used to construct upper layer thickness maps. The location of the BC front is obtained by extracting the 200 m isoline from the altimeter-derived upper layer thickness maps. Errors in the computations associated with the interpolation procedure are larger within the diamond-shaped areas formed by the T/P groundtracks [Goni *et al.*, 1996] and affect the estimates of the frontal locations. Three examples are presented here (Plates 2a–2i) to show the upper layer thickness maps derived from the sea height anomaly maps and to compare the altimeter-derived frontal locations against AVHRR-derived estimates of the sea surface temperature fronts. These maps correspond to January 1995, May 1995, and January 1996. The sea height anomalies exhibit the typical positive-negative alternation at the confluence region off the continental margin, which is primarily due to the motion of the BC front. The locations of the 200 m upper layer thickness contour, or BC front, are shown in white, and the southernmost frontal locations west of  $45^\circ$ W and the separation of the front are indicated with the letters S and F, respectively. These altimeter-derived fronts are compared against estimates from 9 km 8 day AVHRR composites (Plates 2c, 2f, and 2i), where the fronts are obtained from the largest horizontal sea surface gradients associated with the BC front in the confluence region. The 8 day composites were chosen because they exhibit less cloud coverage than the daily images without losing information about the main mesoscale features. These composites show that as expected, the higher sea surface temperatures of the BC are associated with larger upper layer thickness values. There is some disagreement between the AVHRR frontal estimates and the altimeter-derived frontal locations because of the different spatial and temporal sampling, as well as the different definition of the front, used by these two techniques. However, the qualitative agreement is remarkable. Unfortunately, the scarcity of hydrographic observations in the region does not allow comparisons between

hydrographic-derived and altimetric-derived frontal locations to be made.

#### 4.1. Frontal Time Density

The upper layer thickness maps are used to extract the frontal locations (contour line of the 200 m upper layer thickness depth) every 10 days. Closed contours were dismissed in order to include only fronts and not warm rings. The altimeter-derived frontal locations during the 6 year study period, November 1992 to December 1998, exhibit large spatial variability (Figure 4a), which appears to be smaller close to the continental margin. The frontal time density is defined in this study as the number of days each year during the 6 year study period that a front is located within a  $0.25^\circ$  square box. This parameter, obtained from the 200 m contours of the upper layer thickness maps, is used to estimate the mean position of the BC front (Figure 4b). The dotted line in Figure 4 indicates the mean location of the front, as given by the maximum value of the frontal time density along each longitude. The definition of frontal density used here is different than those in previous works [Goni *et al.*, 1996; Garzoli *et al.*, 1992], where the largest sea surface temperature gradient was used to identify the BC front, often associated with the BC jet and not with the BC front. This explains the more zonal distribution of the results presented here. However, the AVHRR-derived frontal positions shown in Plate 2 represent the location of the largest SST gradient associated with the front and not the BC jet and would not have coincided with the BC front found by applying the methodology used by Goni *et al.* [1996] and Garzoli *et al.* [1992]. Other differences can also be attributed to the different spatial and temporal resolution of the data obtained from these two sensors [Morrow and Birol, 1998]. Therefore a direct comparison between frontal positions found here and those computed in previous works is not possible. However, results presented in Figure 4b agree with the mean location of the confluence computed using Geosat altimetry within a wind-driven multilayer model, which was estimated to oscillate between  $36^\circ$  and  $39^\circ$ S [Matano *et al.*, 1993].

#### 4.2. Separation of the Brazil Current Front From the Continental Margin

The separation of the BC front near the continental margin is investigated by locating the BC front along T/P ascending groundtrack a323 (Figure 2). This groundtrack runs almost parallel to the continental margin, although it is sometimes separated up to 200 km from it. The upper layer thickness

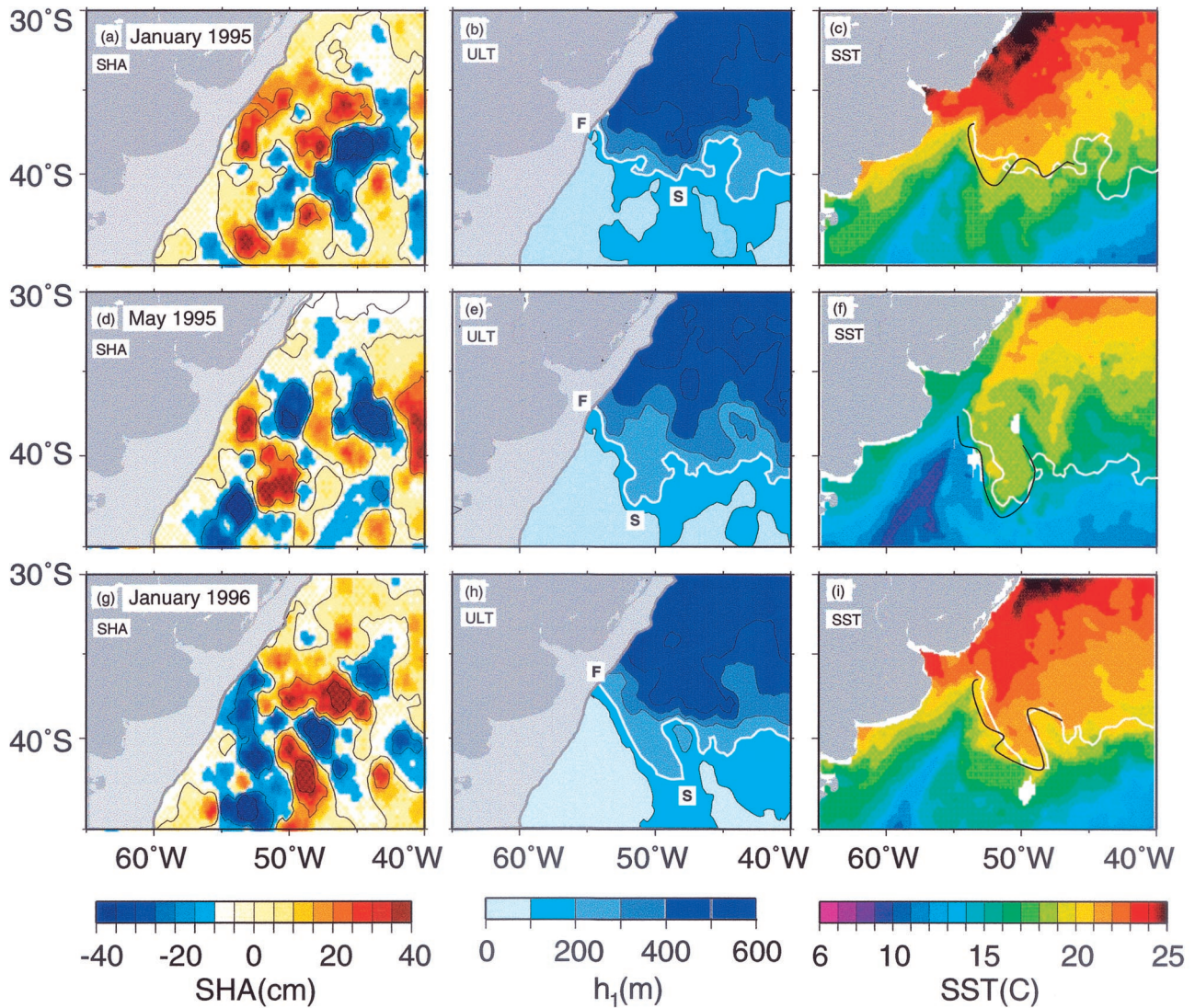


**Plate 2.** (a) T/P-derived sea height anomaly map corresponding to January 9, 1995. (b) Altimeter-derived upper layer thickness for the same date. The light grey area corresponds to the continental shelf. The altimeter-derived front is shown by a white line. The southernmost location of the altimeter-derived front and separation of the front from the continental margin are indicated with S and F, respectively. (c) The 9 km AVHRR-derived sea surface temperature composites for January 1–8, 1995. The black line corresponds to the AVHRR-derived frontal location, while the white line corresponds to the altimeter-derived frontal location. (d) and (e) Same as Plates 2a and 2b except for May 9, 1995. (f) Same as Plate 2c except for May 9–17, 1995. (g) and (h) Same as Plates 2a and 2b except for January 4, 1996. (i) Same as Plate 2c except for January 9–17, 1996.

along this groundtrack, instead of the upper layer thickness fields in the region, is used to estimate the frontal locations to avoid contamination from the interpolation procedure used to obtain the maps. Plate 1c shows the space-time diagram of the altimeter-derived upper layer thickness, the 200 m isoline (yellow line), which represents the approximate location of the separation of the BC from the continental margin, and its mean location (dotted yellow line), which lies south of the location of maximum sea height variability (dotted white line). The time series of the separation (Figure 5a, thin line) reveals that the 6 year mean latitude of separation is  $38.5^{\circ}\text{S}$  with a standard deviation of  $0.8^{\circ}$ . The northernmost excursions of the separation generally occur during the winter and spring months, while the southernmost excursions occur during the

summer and fall months. The amplitude of the oscillations exhibits values as high as  $3^{\circ}$  in latitude. The separation is found north of its mean location (dotted lines in Figure 5a) during most of 1993 and 1997 and south of its mean during 1998, giving an indication of strong year to year variability. The mean annual values and their corresponding standard deviations are shown in the table below Figure 5a. The 6 year mean values found in this study are somewhat to the south of previously derived AVHRR estimates of mean location of separation of the BC front from the continental margin, approximated by the 1000 m isobath, which was estimated to range from  $36^{\circ}$  to  $38^{\circ}\text{S}$ , with a mean value of  $\sim 36.5^{\circ}\text{S}$  [Olson *et al.*, 1988] from late 1981 until mid-1987. This difference is believed to occur because the altimeter groundtrack is to the east where the BC is farther to

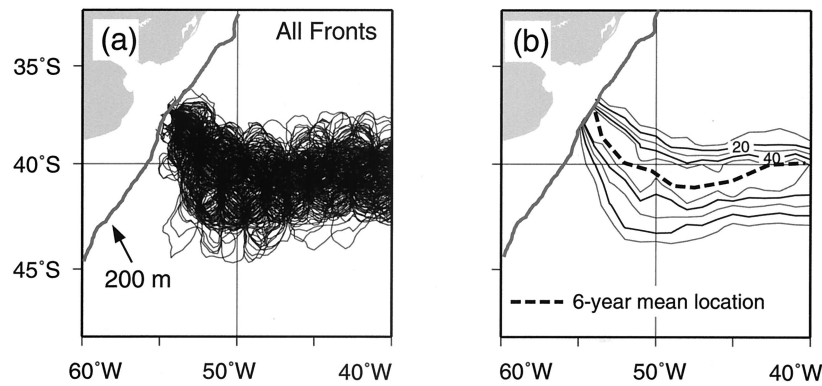


**Figure 4.** (a) Altimeter-derived BC frontal locations from 1993 until 1998. (b) Altimeter-derived annual mean frontal time density maps for the same time period, where the frontal time density is defined as the number of days the fronts are found in a 0.25° square box. The contours are shown in 5 day intervals. The dotted line shows the location of the maximum frontal density values. The 200 m isobath is superimposed on both Figures 4a and 4b.

the south and because of the different definitions of BC front applied in each methodology. The power spectrum corresponding to this time series shows two peaks, at 6 and 12 months, which are significant at the 85% level (Figure 5b). This result agrees with previous studies that have shown that this parameter has a strong annual and semiannual signature [Matano *et al.*, 1993]. The power spectra are computed according to the serial covariance method [Mitchel *et al.*, 1966]. The statistical significance of the power spectra is assessed by assuming the null continuum to be “red noise,” and it is determined by the ratio of the local spectra estimate to be continuum. This ratio is assumed to be redistributed as  $\chi^2/\nu$  [Mitchel *et al.*, 1966], where  $\nu$  is the number of degrees of freedom.

**4.3. Southernmost Frontal Locations**

The variability of the BC fronts is also investigated by extracting the southernmost location west of 45°W of each front. The time series of the longitude and latitude of these locations

are shown in Figures 6a and 6c, respectively. The southernmost location of the BC front oscillates between 52° and 45.5°W and between 41° and 44°S and has a 6 year mean value of 48.6°W and 42.3°S. This parameter has maximum amplitudes with zonal motions of 6° longitude, twice as large as the maximum meridional motions of 3° latitude. The annual amplitude of these two time series ranges from 1° to 6°, denoting a very strong year to year difference. The mean annual values and their corresponding standard deviations for each of these two parameters are listed in the tables below each panel. The power spectra corresponding to these two time series (Figures 6b and 6d) show that the longitude has peaks at 2.5, 3, and 6 months and the latitude also has multiple peaks, at 2, 3, 6, and 12 months, all significant at the 85% level. These results agree with previous estimates from a 1 year long record of inverted echosounder data [Garzoli and Garraffo, 1989]. These estimates are in qualitative agreement with

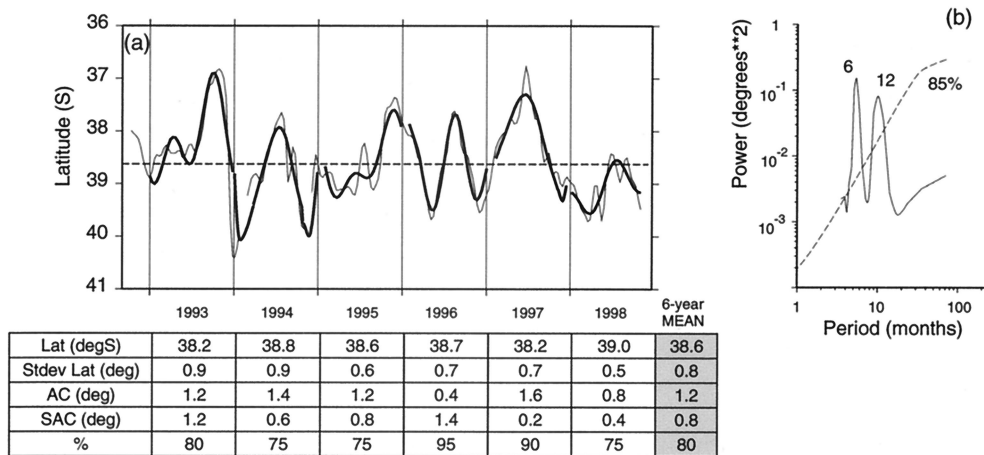


**Figure 5.** (a) Time series (thin lines) and annual plus semiannual fit (thick lines) of the separation of the BC front from near the continental margin as obtained from T/P groundtrack a323. The horizontal dotted line shows the 6 year mean. (b) Power spectrum of the time series showing two peaks, at 6 and 12 months, above the 85% confidence level (dotted line). The table below shows the mean annual value and standard deviation of each parameter, the amplitude of the annual (AC) and semiannual (SAC) cycles of each time series during each year, and the percentage of variability explained by these two cycles. The shaded column shows the 6 year mean values.

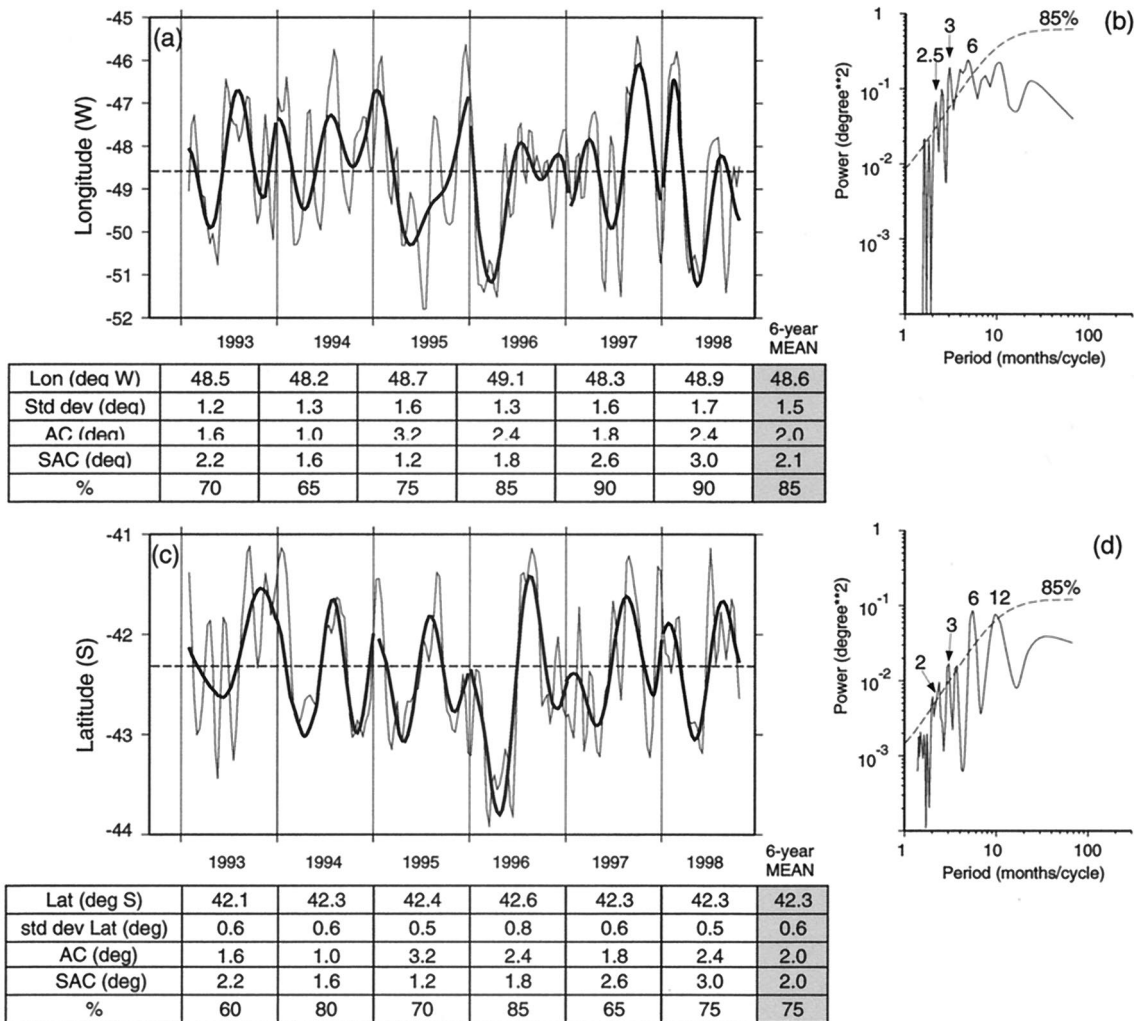


**Figure 6.** Time series (thin lines) and annual plus semiannual fit (thick lines) of the (a) longitude and (c) latitude of the altimeter-derived southernmost location of the BC front. (b) and (d) Power spectrum of time series for Figures 6a and 6c, respectively, showing the 85% confidence level (dotted line). The tables below each panel show the mean annual value and standard deviation of each parameter, the amplitude of the annual (AC) and semiannual (SAC) cycles of each time series during each year, and the percentage of variability explained by these two cycles. The shaded column in each table shows the 6 year mean values. The horizontal dotted lines in Figures 6a and 6c are the 6 year mean values.

inverted echo sounder (IES)-derived results obtained by *Garzoli and Simionato* [1990] during the June 1985 to March 1986 time period and are within the range of AVHRR-derived results that showed the surface BC front to have a location ranging from  $37^{\circ}$  to  $46^{\circ}$ S during September 1975 to April 1976 [*Legeckis and Gordon*, 1982].

#### 4.4. Transports

The transport time series of the BC and MC are used in this study to investigate possible correlations between these two currents and the frontal parameters analyzed in the sections above. Plate 1e shows the space-time diagram of sea height anomaly for descending groundtrack *d294* (Figure 2). The largest value of rms sea height is located at  $\sim 40^{\circ}$ S (Plate 1d), similar to the mean location of the front, which is at  $41^{\circ}$ S. The time series of the frontal location (yellow line in Plate 1f) shows that the front is always located south of  $38^{\circ}$ S along this same groundtrack. The BC transport is estimated in this study by computing the individual southward contributions of water

mass transport across the T/P descending groundtrack *d294* using (3) and between the 200 m isobath and  $38^{\circ}$ S. The step in which these individual contributions are computed is given by the T/P alongtrack resolution, which is 9 km. The time series of the BC transport (Figure 7a) reveals that its values range between 5 and 25 Sv, with a 6 year mean of 14 Sv (dotted line in Figure 7a) and a standard deviation of 7 Sv. The power spectrum corresponding to this time series shows multiple peaks, at 3, 6, and 12 months, which are significant at the 85% level (Figure 7b). The time series of BC transport exhibits a rather strong year to year variability, where the mean transports during 1996 and 1997 are 50% larger than during 1995.

The time series of the MC transport used in this work was computed using a combination of current meter and altimetry data (*Vivier et al.*, submitted manuscript, 2001). This time series shows that the power spectrum of the MC transport exhibits two main peaks. The first peak, at 180 days, reflects a barotropic adjustment of this current to changes in the wind

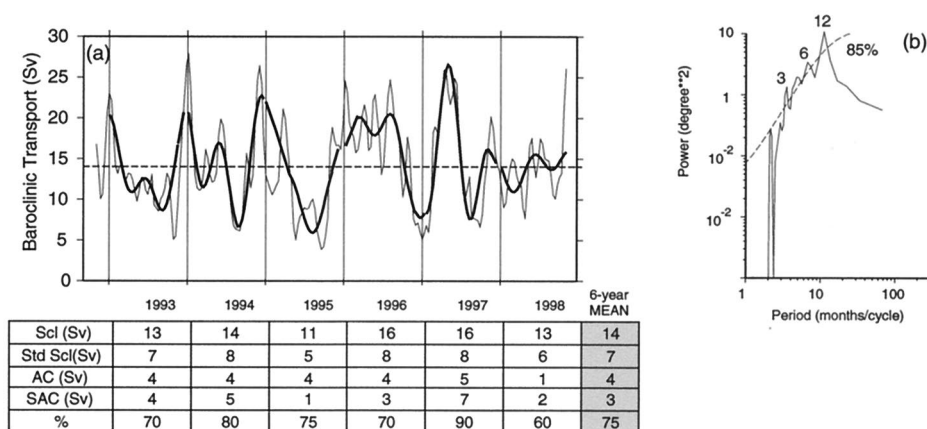


**Figure 7.** (a) Time series (thin lines) and annual plus semiannual fit (thick lines) of the altimeter-derived BC baroclinic transport across T/P groundtrack  $d294$ . The horizontal dotted line is the six year mean value. (b) Power spectrum of the time series showing peaks, at 3, 6, and 12 months, above the 85% confidence level (dotted line). The table below shows the mean annual value and standard deviation of this parameter, the amplitude of the annual (AC) and semiannual (SAC) cycles of the time series during each year, and the percentage of variability explained by these two cycles. The shaded column shows the 6 year mean values.

stress curl. The second one, at 70 days, is associated with shelf wave propagation in the continental margin.

## 5. Discussion

The annual (AC) and semiannual (SAC) components of the four time series discussed in the previous sections are investigated here by fitting two sine functions with annual and semiannual periods (thick lines in Figures 5–7). The amplitudes of these two components, shown in the third and fourth rows of the tables in Figures 5–7, reveal that they can be used to describe most of the variability of these parameters, with the remainder of the signal including the signal due to ring shedding by the BC.

The time series of the separation of the BC front has mean annual values that exhibit weak year to year variability (table in Figure 5). However, the annual mean amplitudes have very large year to year variations, with the annual standard deviations indicative of the large variability present in timescales shorter than a year. The time series of this parameter has a very strong annual component, which, together with the semiannual component, explains from 75 to 95% of the variability every year. The amplitudes of these components vary from year to year, ranging from  $0.2^\circ$  to  $1.6^\circ$  (Figure 5a).

The latitude and longitude of the southernmost location of the front also exhibits annual and semiannual components with strong year to year variability. In the 6 year mean (shaded boxes in tables of Figure 6) both components appear to be of the same order of magnitude, although the annual component of the longitude is not significant at the 85% level (Figure 6b). The AC and SAC account for more than 75 and 85% of variability of the longitude and latitude of the southernmost frontal locations, respectively. The release of warm-core rings by the BC probably represents the main source of year to year variability of these two parameters, as 4–9 rings are shed every year by this current (Lentini et al., submitted manuscript, 2001).

The BC transport exhibits an annual component slightly larger than the semiannual component, which together account for 75% of the transport variability (Figure 7). The year

to year variability of the BC transport is observed in the amplitude of the AC and SAC values, which explain  $\sim 75\%$  of the variability.

A coherence analysis is used to investigate the frequencies at which the BC and MC transports are best correlated with the latitude of separation of the BC front and with the latitude of the southernmost BC frontal location (Figures 8a–8d). The coherence is a normalized measure of the equality of the power spectra of the two signals in the frequency domain within a specified frequency band. A coherence peak at 6 months is obtained between the BC and MC and the latitude of separation (Figures 8a and 8c, respectively), where the coherence confidence limit [Emery and Thompson, 1998] is 0.62 at 70% confidence level. This 6 month peak has been shown to be associated with the barotropic adjustment to changes in the wind stress curl in the South Pacific (Vivier et al., submitted manuscript, 2001). Slightly different results are found for the coherence between these two currents and the latitude of the southernmost location of the BC front, where, besides the 6 month peak, there is a peak at 3 months (Figures 8b and 8d), also significant at the 70% level. These results stress the importance of the semiannual transport signal. Although these parameters and the transport time series of the BC and MC clearly have annual as well as semiannual components, the coherences between these two currents and the frontal parameters are only significant at the semiannual and shorter periods.

The seasonal variability of these same parameters is investigated by computing the altimeter-derived mean monthly values for the entire 6 year record, shown in Figures 9a–9d, with positive anomalies from their annual means denoted by lighter shading. During the austral summer and fall seasons the monthly means of the BC transport exhibit values larger than the annual mean of 14 Sv, while during the winter and early spring seasons these mean transport values fall below the annual mean (Figure 9a), indicative of a strong annual cycle. The mean standard deviation of the mean monthly BC transport values, a measure of the uncertainty of these estimates, is  $\sim 4$  Sv. These results agree with estimates obtained from inverted

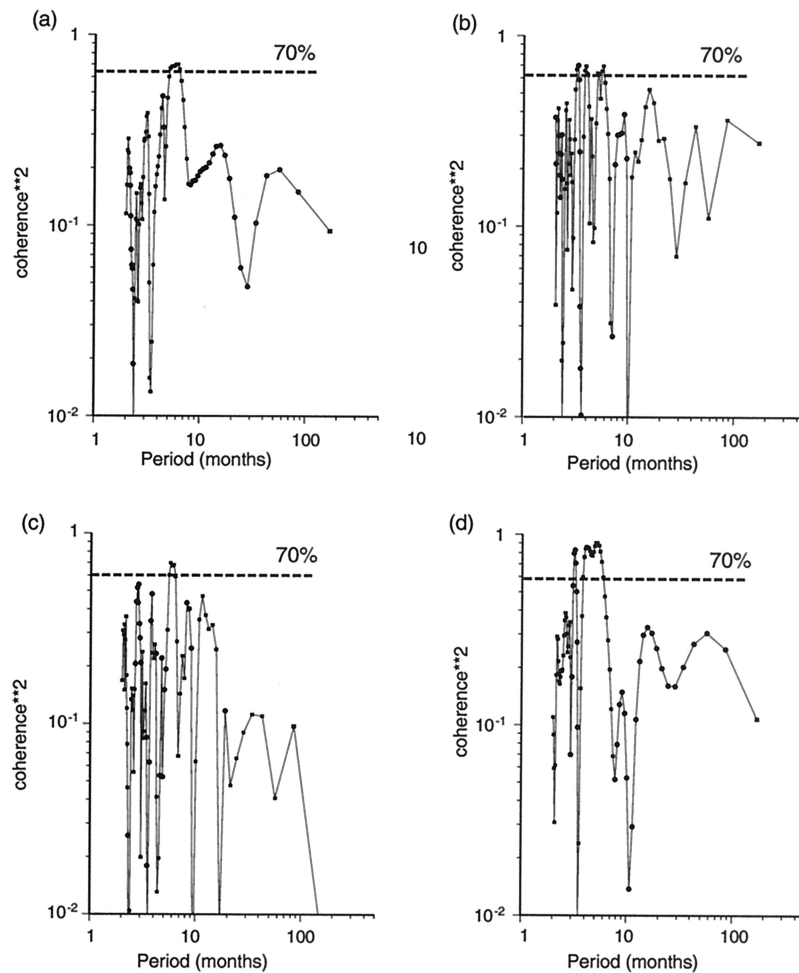


**Figure 8.** Coherence spectra between the altimeter-derived BC transport and (a) the separation of the BC front and (b) the southernmost BC frontal location and between the altimeter-derived MC transport and (c) the separation of the BC front and (d) the southernmost BC frontal location. The dotted horizontal lines indicate the coherence confidence limit at 70%.

echosounder and Geosat altimeter data [Goni *et al.*, 1996], from Geosat and wind data incorporated into a dynamic model [Matano *et al.*, 1993], and from other reported transport estimates [Maamaatuaiahutapu *et al.*, 1998]. The monthly mean MC transport time series is shown in Figure 9b. The minimum transport values occur during the months of April and September, and the maximum occur during the months of June and November, an indication of its strong semiannual component. The mean standard deviation of the mean monthly values of the MC transport is  $\sim 5$  Sv. The mean monthly estimates of the latitude of the separation of the BC front from the continental margin (Figure 9c) indicate that the separation exhibits northern excursions during the winter and spring months and southern excursions during the summer and fall months. The standard deviation of the mean monthly values is  $\sim 0.2^\circ$ . The mean monthly estimates of the latitude of the southernmost location of the BC front (Figure 9d) reveal that the fronts exhibit extreme southern motions during March (fall), May (fall), and October (late spring). The northern excursions of the front are found during the summer, winter, and early spring, with peaks during January (summer) and August (winter). The mean standard deviation of the mean monthly values is  $\sim 0.5^\circ$ .

The influence of the BC and MC transports on the BC frontal motion can be also investigated by analyzing if these currents may trigger, or at least be linked to, a southward or northward movement of the separation of the BC front from the continental margin. We investigate here the relationship between the deviation of the frontal motion and of the transport of the BC and MC from their 6 year mean value (Figures 9a–9d). During the summer, fall, winter, and early spring months, positive (negative) anomalies of the BC transport appear to be related to negative (positive) anomalies of latitudes of separation and southernmost location. However, during late spring the relationship appears to be linked to the variations of these parameters instead, as increases in transport values still correspond to southern excursions of the latitude of separation but to northern movements of the southernmost location.

Five separate cases are examined here linking the monthly mean time series of the transport values of the BC and MC (Figures 9a and 9b) to the location of separation of the BC (Figure 9c) and to the southernmost frontal location (Figure 9d). These five cases correspond to the same number of episodes, shown here as cases A–E, in which the latitude of separation exhibits a relative maximum or minimum (solid circles), denoting the beginning of a shift toward the south or

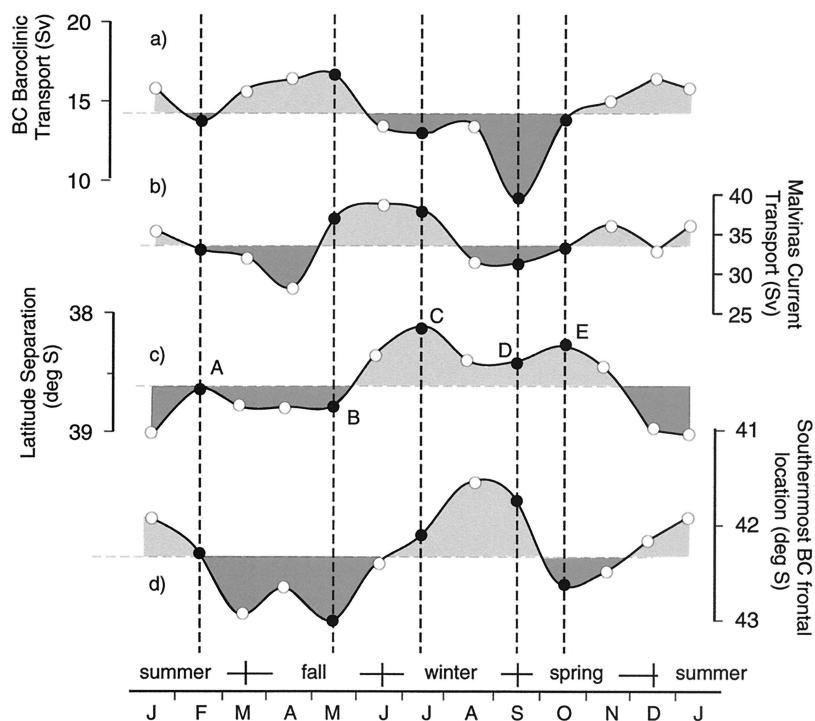


**Figure 9.** Mean monthly values (circles) of the altimeter-derived (a) baroclinic transport of the BC across T/P groundtrack *d294*, (b) transport of the MC, (c) latitude of the southernmost location of the BC, and (d) latitude of the separation of the BC front from the continental margin, as detected by ascending T/P groundtrack *a323*. The horizontal dotted lines are placed at the mean annual values of each parameter, and a smooth line linking the open circles is superimposed. Positive (negative) anomalies of each parameter with respect to the annual mean is indicated by light (dark) shading. Five events (A–E) associated with a maximum or minimum of the separation time series are shown in solid circles.

north of the separation point. Case A (February) shows that as the BC transport begins to increase and the MC transport decreases, the separation and southernmost locations move south. Case B (May) shows that when the BC transport starts decreasing and the MC transport remains unchanged, the separation and southernmost locations begin moving north. Case C (July) shows that when the BC transport remains almost unchanged and the MC transport starts decreasing, the separation begins going south, while the southernmost location moves northward. Case D (September) shows that when the BC and MC transports start increasing, the separation remains almost unchanged, and the southernmost location moves south. Case E (October) shows that when both the BC and MC transports increase, the separation begins going toward the south, and the southernmost location starts moving north. Although the 6 year mean can only provide a very crude reference for investigating this relationship, results obtained here suggest that although the transport anomalies are linked to the frontal movement, relative maximum or minimum values in BC transport dominate the movement of the latitude of separation, except during late spring and early summer when both current transports increase and the frontal separation goes to the north. Similarly, the relationship between the variability of these two current transports shows a link with the southernmost location of the BC front, where increases (decreases) in the BC transport are related to a southward (northward) movement of the front, except during the spring months. A positive anomaly in the location of the separation of the front corresponds with a positive anomaly in the southernmost lo-

cation during the fall and winter months. However, during spring (summer) a northern (southern) anomaly of the separation corresponds to a southern (anomaly) of the front. Although the existence of a link or correlation does not explicitly denote a cause or effect, this result confirms the hypothesis brought by *Vivier and Provost* [1999] that the MC may play a marginal role in the annual component of the BC frontal motion, which appears to be dominated by the BC transport (*Vivier et al.*, submitted manuscript, 2001).

## 6. Conclusions

This research presents for the first time a methodology to monitor the BC frontal motions using altimeter-derived sea height anomaly data within a two-layer reduced gravity ocean dynamical model. This scheme allows the study of frontal movements over a period of 6 years, from 1993 until 1998, which enables investigation of the year to year variability of the BC front and transport. Despite the difference in spatial and temporal resolution the altimeter-derived frontal maps agree with previous remote sensing estimates and model results, demonstrating its ability to monitor subsurface dynamics. Results obtained in this research reveal that the 6 year mean location where the fronts separate from the continental margin (approximated by an ascending T/P groundtrack) is  $38.6^{\circ}\text{S}$ , with marked annual and semiannual cycles. The motions of the southernmost intrusions of the BC fronts exhibit larger zonal ( $6^{\circ}$ ) than meridional ( $3^{\circ}$ ) excursions, with the mean southernmost location of the BC front during the study period corre-

sponds to 42.3°S. The BC front exhibits motions that have dominant periods of 75, 90, and 180 days meridionally and 60, 90, 180, and 360 days zonally. The separation of the BC from the continental margin has dominant periods at 180 and 360 days meridionally. The estimates of the BC transport range from 5 to 25 Sv. The mean annual baroclinic transport of the BC across descending T/P groundtrack *d*294 ranges between 11 and 16 Sv, with a standard deviation of 7 Sv and a 6 year mean of 14 Sv. While the MC has peaks at 70 and 180 days [Vivier *et al.*, 2001], this study shows the BC exhibits dominant peaks at 90, 180, and 360 days. Results from coherence analysis show that the frontal displacements have a correlation with the BC and MC transports in periods of 3 and 6 months. In general, relative maximum values in the BC transport are linked to a southward movement of the BC front and a shift to the south of the BC frontal separation from the continental margin, except during the spring months. Although the methodology applied here shows a link between the transport of the currents and the frontal movement, the use of theoretical models is necessary to investigate the trigger mechanisms of the frontal motions. Future studies using the methodology described herein will involve the investigation of the warm rings shed at the BC and their relationship with BC transport fluctuations.

**Acknowledgments.** This research was supported by NOAA/AOML (G. Goni) and by a Brazilian government grant (CNPq 300223/RN, I. Wainer). The authors gladly recognize the help provided by S. Garzoli and E. Johns (NOAA/AOML) during the early part of the writing of this manuscript. The altimeter data were provided by Robert Cheney (NOAA/NESDIS). The authors want to thank Christine Provost and Frederic Vivier for providing the time series of the MC transport. J. Trinanes-Fernandez provided help with the AVHRR imagery.

## References

- Agra, C., and D. Nof, Collision and separation of boundary currents, *Deep Sea Res., Part 1*, 40, 2259–2282, 1993.
- Cheney, R., L. Miller, R. Argreen, N. Doyle, and J. Lillibridge, TOPEX/Poseidon: The 2-cm solution, *J. Geophys. Res.*, 99, 24,555–24,564, 1994.
- Confluence Principal Investigators, CONFLUENCE 1988–1990: An intensive study of the southwestern Atlantic, *Eos Trans. AGU*, 71, 1131–1134, 1990.
- Conkright, M. E., et al., World ocean database 1998, *Natl. Oceanogr. Data Cent. Internal Rep. 14*, 113 pp., U.S. Dep. of Comm., Washington, D. C., 1998.
- Emery, W., and R. Thompson, *Data Analysis Methods in Physical Oceanography*, 634 pp., Pergamon, New York, 1998.
- Garfield, N., The Brazil Current at subtropical latitudes, Ph.D. diss., 122 pp., Univ. of R. I., Kingston, 1990.
- Garzoli, S. L., and A. Bianchi, Time-space variability of the local dynamics of the Malvinas-Brazil Confluence as revealed by inverted echo sounders, *J. Geophys. Res.*, 92, 1914–1922, 1987.
- Garzoli, S. L., and Z. Garraffo, Transports, frontal motions and eddies at the Brazil-Malvinas Currents confluence, *Deep Sea Res., Part A*, 36, 681–703, 1989.
- Garzoli, S. L., and C. Simionato, Baroclinic instabilities and forced oscillations in the Brazil/Malvinas Confluence front, *Deep Sea Res., Part A*, 37, 1053–1074, 1990.
- Garzoli, S. L., Z. Garraffo, G. Podesta, and O. Brown, Analysis of a general circulation model product, 1, Frontal systems in the Brazil/Malvinas and Kuroshio/Oyashio regions, *J. Geophys. Res.*, 97, 20,117–20,138, 1992.
- Goni, G. J., S. Kalmholtz, S. L. Garzoli, and D. B. Olson, Dynamics of the Brazil-Malvinas Confluence based upon inverted echosounders and altimetry, *J. Geophys. Res.*, 101, 16,273–16,289, 1996.
- Gordon, A. L., South Atlantic thermocline ventilation, *Deep Sea Res., Part A*, 28, 1239–1264, 1981.
- Gordon, A. L., Brazil-Malvinas Confluence—1984, *Deep Sea Res., Part A*, 36, 359–384, 1989.
- Gordon, A. L., and C. L. Greengrove, Geostrophic circulation of the Brazil-Falkland Confluence, *Deep Sea Res., Part A*, 33, 573–585, 1986.
- Large, W. G., and H. van Loon, Large scale, low frequency variability of the 1979 FGGE surface buoy drifts and winds over the Southern Hemisphere, *J. Phys. Oceanogr.*, 19, 216–232, 1989.
- Lebedev, I., and D. Nof, The drifting confluence zone, *J. Phys. Oceanogr.*, 26, 2429–2448, 1996.
- Legeckis, R., and A. L. Gordon, Satellite observations of the Brazil and Falkland Currents—1975 to 1976 and 1978, *Deep Sea Res., Part A*, 29, 375–401, 1982.
- Lentini, C. A. D., G. G. Podesta, E. J. D. Campos, and D. B. Olson, Sea surface temperature anomalies on the western South Atlantic from 1982 to 1994, *Cont. Shelf Res.*, 21, 89–112, 2001.
- Levitus, S., Climatological atlas of the world, *NOAA Prof. Pap. 13*, 173 pp., U.S. Dep. of Comm., Washington, D. C., 1982.
- Maamaatuaiahutapu, K., V. C. Garcon, C. Provost, M. Boulahdid, and A. P. Osiroff, Brazil-Malvinas confluence: Water mass composition, *J. Geophys. Res.*, 97, 9493–9505, 1992.
- Maamaatuaiahutapu, K., V. C. Garcon, C. Provost, and H. Mercier, Transports of the Brazil and Malvinas Currents at their confluence, *J. Mar. Res.*, 56, 417–438, 1998.
- Matano, R. P., On the separation of the Brazil Current from the coast, *J. Phys. Oceanogr.*, 23, 79–90, 1993.
- Matano, R. P., M. G. Schlax, and D. B. Chelton, Seasonal variability in the southwestern Atlantic, *J. Geophys. Res.*, 98, 18,027–18,035, 1993.
- Mitchel, J. M., B. Dzerdzeevski, H. Flohn, W. L. Hofmeyer, H. H. Lamb, K. N. Rao, and C. C. Wallen, Climatic change, *Tech. Rep. 79*, World Meteorol. Org., Geneva, Switz., 1966.
- Morrow, R. A., and F. Birol, Variability in the southeast Indian Ocean from altimetry: Forcing mechanisms for the Leeuwin Current, *J. Geophys. Res.*, 103, 18,529–18,544, 1998.
- Olson, D. B., G. P. Podesta, R. H. Evans, and O. B. Brown, Temporal variations in the separation of the Brazil and Malvinas Currents, *Deep Sea Res., Part A*, 35, 1971–1990, 1988.
- Piola, A. R., E. J. D. Campos, O. O. Moller, M. Charro, and C. Martinez, The subtropical shelf front off eastern South America, *J. Geophys. Res.*, 105, 6565–6578, 2000.
- Provost, C., and P.-Y. Le Traon, Spatial and temporal scales in altimetric variability in the Brazil-Malvinas Confluence region: Dominance of semiannual periods and large spatial scales, *J. Geophys. Res.*, 98, 18,037–18,062, 1993.
- Provost, C., O. Garcia, and V. Garcon, Analysis of satellite sea surface temperature time series in the Brazil-Malvinas Current confluence region: Dominance of the annual and semiannual periods, *J. Geophys. Res.*, 97, 17,841–17,858, 1992.
- Roden, G. I., Thermohaline fronts and baroclinic flow in the Argentine Basin during the austral spring of 1984, *J. Geophys. Res.*, 91, 5075–5093, 1986.
- Sunye, P. S., and J. Servain, Effects of seasonal variations in meteorology and oceanography on the Brazilian sardine fishery, *Fish. Oceanogr.*, 7, 89–100, 1998.
- Vivier, F., and C. Provost, Volume transport of the Malvinas Current: Can the flow be monitored by TOPEX/Poseidon?, *J. Geophys. Res.*, 104, 21,105–21,122, 1999.
- Wainer, I., P. Gent, and G. Goni, The annual cycle of the Brazil-Malvinas Confluence region in the NCAR climate system model, *J. Geophys. Res.*, 105, 26,167–26,177, 2000.

G. J. Goni, Atlantic Oceanographic and Meteorological Laboratory, National Oceanic and Atmospheric Administration, U.S. Department of Commerce, 4301 Rickenbacker Causeway, Miami, FL 33149, USA. (goni@aoml.noaa.gov)

I. Wainer, Physical Oceanography Department, Universidade de Sao Paulo, Proco do Oceanografico 191, 05508-900 Sao Paulo, Brazil.

(Received April 27, 2000; revised April 24, 2001; accepted May 17, 2001.)